Reduced Diffusion Encoding for Accurately Estimating Axonal Injury, Demyelination, and Inflammation in Mouse Optic Nerve

Chia-Wen Chiang[1], Yong Wang[2], Anne H. Cross[3,4], and Sheng-Kwei Song[2,4]

[1]Chemistry, Washington University, Saint Louis, MO, United States, [2]Radiology, Washington University School of Medicine, Saint Louis, MO, United States, [3]Neurology, Washington University School of Medicine, Saint Louis, MO, United States, [4]The Hope Center for Neurological Disorders, Washington University School of Medicine, Saint Louis, MO, United States

Introduction

Diffusion tensor imaging (DTI) has been successfully used to detect axon/myelin dysfunction in white matter injury [1]. However, the Gaussian diffusion assumption hampered its application to quantify non-Gaussian characters. Many new diffusion MRI techniques, such as generalized DTI (gDTI) [2], diffusion spectrum imaging (DSI) [3], diffusion kurtosis imaging (DKI)[4], composite hindered and restricted model of diffusion (CHARMED) [5], have been proposed to model the non-Gaussian diffusion in the past decade. We have recently developed a new diffusion MRI method, diffusion basis spectrum imaging (DBSI), to resolve crossing fibers and quantify confounding effects of inflammation [6]. A 99-direction diffusion-encoding scheme was employed for acquiring DBSI data providing sufficient information to accurately detect and quantify multiple diffusion components including crossing fibers, axonal injury, demyelination, and inflammation in both ex vivo phantom and an in vivo animal model [6]. However, the initial DBSI protocol with 99-direction diffusion weighting scheme leads to a lengthy scanning time. To image small coherent white matter tract such as mouse optic nerve, high spatial resolution and high SNR are required, significantly hampering in vivo DBSI applications. Taking the advantage of the simple structure of optic nerve without crossing fibers, we removed the redundancy in the original 99-direction DBSI diffusion weighting scheme in this study. We demonstrated that a simplified 29-direction DBSI diffusion weighting scheme was adequate to generate DBSI results from mouse optic nerves that were comparable to those obtained using the full 99-direction diffusion-encoding scheme.

Method _99-direction DBSI scheme:_ Standard 99 DBSI diffusion-encoding directions can be visualized on a 3D Cartesian grid system (blue boxes in Figure 1). Each diffusion-encoding vector starts from the origin of the Cartesian grid system and ends at a non-origin grid point (colored arrows) including (1) 93 diffusion-encoding vectors located inside the sphere of radius = 3 and (2) 6 diffusion-encoding vectors located at the crossing points between the Cartesian axes and the sphere which constitutes the 99-direction DBSI diffusion-encoding scheme. DBSI diffusion-encoding scheme is the same as the grid scheme used in DSI [3]. However, DBSI only uses the inner part of the DSI grid scheme. The maximal diffusion weighting factor (b-value) of DBSI scheme was 3200 s/mm^2 for ex vivo studies.

Simplified 29-direction DBSI scheme: The simplified 29-direction diffusion weighting scheme (blue arrows with red circles at the tip in Figure 2) was selected and derived from the original 99-direction scheme (blue arrows in Figure 1) by removing symmetric or redundant diffusion-encoding directions while maintaining the diffusion space well sampled and the b-value fully distributed from the range of 0 to 3200 s/mm^2 for ex vivo studies.

DBSI scan of fixed optic nerves of experimental autoimmune encephalomyelitis (EAE)-affected mice: Five fixed, female EAE-affected C57BL/6 mouse brains with individual paired optic nerves, four mice at acute stage and one at chronic stage with severe pathologies, were examined with both 99- and 29-direction DBSI at the same experimental setup on a 4.7 Tesla scanner using multiple-echo spin-echo sequence [7] with the following parameters: TR 1.2 s, TE 38 ms, Δ 15 ms, δ 5 ms, field-of-view 20 mm × 20 mm, data matrix 256 × 256 (before zero-filled), slice thickness 1 mm, 1 average, and maximal b-value 3200 s/mm^2. Total acquisition time for 99- and 29-direction DBSI was 8 h 25 min and 2 h 30 min respectively. Voxel-based analysis was performed on non-zero filled 99- and 29-direction DBSI data, 50 voxels from 10 optic nerves were used for comparison.

DBSI analysis: Eq. [1] was solved by fitting the 99 (or 29) diffusion weighted signals using a linear combination of diffusion basis sets consisting of cylindrically symmetric diffusion tensors [3] with the freedom to vary $\lambda_{||}$ and $\lambda_\perp$ to estimate the number of anisotropic diffusion tensor components (N_{aniso}) and the associated principal directions. After N_{Aniso} was computed, the number of isotropic component (N_{iso}) was further determined using nonnegative least-squares (NNLS) analysis. The global nonlinear optimization was conducted employing direct pattern search to solve Eq. [1]. S_k is the kth measured diffusion weighted signals (k = 1, 2, 3, …). S_i and S_j are fractions of anisotropic diffusion components and isotropic diffusion component respectively.
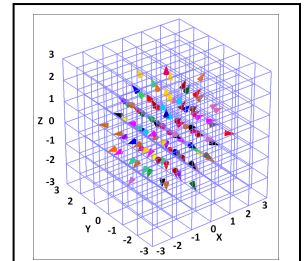

Figure 1 Original 99-direction scheme. Each diffusion-encoding vector starts from the origin of the Cartesian grid system and ends at a non-origin grid point (colored arrows).
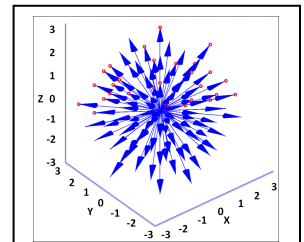

Figure 2 New 29-direction scheme (blue arrows with red marks) is simplified from the 99-direction scheme (blue arrows).
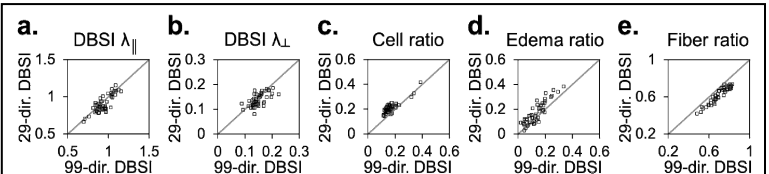
$$S_k = \sum_{i=1}^{N_{Aniso}} S_i e^{-\left|\vec{b}_k\right|\lambda_\perp} e^{-\left|\vec{b}_k\right|(\lambda_{||} - \lambda_\perp) cos^2\theta_i} + \sum_{j=1}^{N_{iso}} S_j e^{-\left|\vec{b}_k\right| d_j} \quad [1]$$

Figure 3 29- and 99-direction DBSI indices distributed close to the line of identity, indicating minor offsets using 29-direction scheme.

Results and Discussion

Scatter plots (Fig. 3 a-e) qualitatively revealed that most data points distributed near the line of identity with small offsets. Bland-Altman analysis (Table 1) quantitatively suggested that 29- and 99-direction DBSI indices were comparable with acceptable standard deviations of the difference and small biases. For the animal tissues demonstrated in this study, the scanning time was reduced by 2/3rds using the simplified 29-direction DBSI compared to the original 99-direction scheme. The same spatial resolution and DBSI computation accuracy was maintained for mouse optic nerves ex vivo. Currently, by employing single-shot diffusion-weighted EPI, 99-direction DBSI with 2 x 2 x 2 mm^3 resolution can be acquired within 15 min on a 3.0 Tesla Trio TIM (Siemens, Erlangen, Germany) human scanner. If the same 2 x 2 x 2 mm^3 resolution is maintained, the simplified 29-direction scheme will shorten the scanning time to 5 minutes.

DBSI Indices		DBSI $\lambda_{||}$	DBSI $\lambda_\perp$	Cell ratio	Edema ratio	Fiber ratio
Mean (±S.D.)	29-dir.	0.91 (±0.11)	0.14 (±0.03)	0.21 (±0.05)	0.17 (±0.09)	0.62 (±0.09)
	99-dir.	0.94 (±0.10)	0.15 (±0.03)	0.16 (±0.05)	0.13 (±0.07)	0.70 (±0.09)
29-dir. vs. 99-dir.	Bias[1]	-0.04	-0.01	0.04	0.04	-0.08
	Precision[2]	0.06	0.02	0.03	0.04	0.03

[1] Bias = average difference of Bland-Altman plot of 29- minus 99-direction DBSI against mean;
[2] Precision = 1 S.D. of difference; directional diffusivity in μm^2/ms.

Table 1 Quantitative Bland-Altman analysis of the simplified 29- and original 99-direction DBSI, indicating good agreement between the two schemes.

References [1] Song, SK. _et al. Neuroimage_ 2002; 17:1429 . [2] Chunlei L. _et al. MRM_ 2004; 51:924–937; [3] Wedeen, VJ. _et al. Neuroimage_ 2008; 41:1267-77; [4] Fieremans, E. _et al. Neuroimage_ 2011; 58:177-188; [5] Assaf,Y. _et al. Neuroimage_ 2005; 27: 48-58; [6] Wang,Y. _et al. Brain_ 2011, 134:3590; [7] Tu TW. _et al. Proc. Intl. Soc. Magn. Reson. Med._ 18 (2010), 4001.